Positive-Contrast Imaging with Phase-Perturbed Differenced SSFP

R. R. Ingle[1], and D. G. Nishimura[1]
[1]Electrical Engineering, Stanford University, Stanford, California, United States

Introduction: Several fast, steady-state imaging techniques have recently been developed for positive-contrast imaging of superparamagnetic iron-oxide (SPIO) nanoparticles as a means of tracking labeled cells [1-4]. These methods enable rapid imaging with high SNR efficiency but have limited background suppression [1], limited or motion-sensitive fat suppression [2], or limited resolution [3,4]. In this work, we present a novel Phase-Perturbed Differenced Steady-State Free Precession (PDSSFP) sequence achieving high peak positive contrast and motion-insensitive water and fat suppression. We compare the contrast-to-noise ratio (CNR), peak contrast (C), and spectral profile of PDSSFP with several steady-state positive-contrast sequences using Bloch simulations and phantom scans.

Theory and Methods: The PDSSFP pulse sequence is obtained by perturbing alternate RF phases of a balanced SSFP (bSSFP) sequence by $\Delta\phi$ degrees and acquiring two interleaved acquisitions during even and odd repetition times (TRs) (Fig. 1). The phase perturbation yields an oscillating steady-state magnetization profile having large deviations from the bSSFP profile in the passband but little change in the transition band. By subtracting even- and odd-TR acquisitions, the resulting magnitude profile contains large peaks at the bSSFP passband frequencies and nulls at the transition-band frequencies. With the choice of TR=4.8 ms and $\Delta\phi$=10°, nulls are centered on water and fat resonances at 1.5T. Bloch simulations were performed to compare the spectral profiles of low-flip-angle bSSFP (FLAPS [1]), low-flip-angle ATR ($PARTS_{ws}$ [2]), product of water-suppressed (ws) and fat-suppressed (fs) PARTS ($PARTS_{comb}$ [2]), and PDSSFP (Fig. 2). Flip angles were chosen to maximize CNR (defined in [2] as difference between mean off- and on-resonant signal), yielding 5°, 15°, and 40° for FLAPS, PARTS, and PDSSFP, respectively. PDSSFP achieves the highest peak contrast (defined in [2] as ratio of peak off-resonant to mean on-resonant signal) at these flip angles (Fig. 3).

Results: Spectral profiles of PARTS and PDSSFP were verified by scanning a uniform spherical phantom with a linear field gradient (Fig. 4). $PARTS_{ws}$ and $PARTS_{fs}$ were multiplied to suppress both water and fat, but the resulting image is potentially sensitive to inter-scan motion. PDSSFP component images were subtracted to yield the PDSSFP profile, which is robust to motion due to the inherent interleaved acquisition strategy. A gel phantom (4% agar, 8mM $NiCl_2$) with four cylindrical wells containing 100, 200, 400, and 800 µg/mL solutions of SPIO nanoparticles (Chemicell, Berlin, Germany) was constructed. Phantom experiments were performed on a GE 1.5T scanner using a birdcage head coil. 3D GRE (TR=22 ms, TE=5 ms, α=30°), FLAPS (TR=4.8 ms, α=5°), PARTS (TR_1=3.9 ms, TR_2=0.9 ms, α=15°), and PDSSFP (TR=4.8 ms, α=40°, $\Delta\phi$=10°) images were acquired with a 14 cm FOV, 0.7x0.7x1 mm^3 resolution, and scan times of 1:04s (FLAPS, $PARTS_{ws,fs}$) and 2:07s ($PARTS_{comb}$, PDSSFP). PDSSFP achieves good water and fat suppression via a robust interleaved acquisition technique.

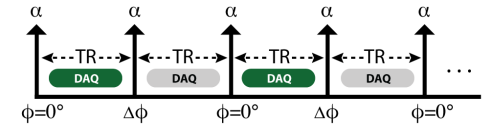

Figure 1. PDSSFP pulse sequence diagram. Alternate RF phases perturbed by $\Delta\phi$ degrees. Interleaved signal acquisition during even and odd TRs.

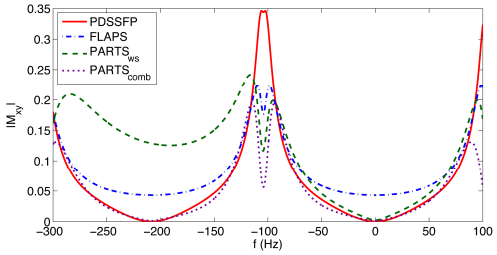

Figure 2. Magnetization profiles for PDSSFP (α=40°, $\Delta\phi$=10°, TR=4.8 ms), FLAPS (α=5°, TR=4.8 ms), $PARTS_{ws}$ (α=15°, TR_1=3.9 ms, TR_2=0.9 ms), and $PARTS_{comb}$. PDSSFP has high peak contrast and nulls centered on water and fat resonances. (T1/T2=5)

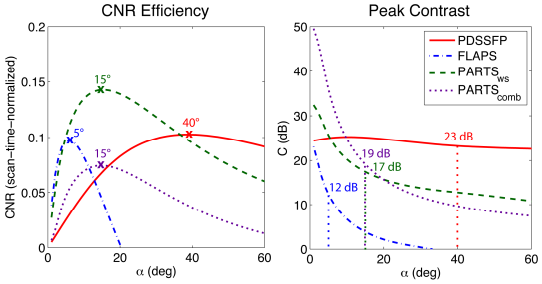

Figure 3. Optimal flip angles for PDSSFP, FLAPS, $PARTS_{ws}$, and $PARTS_{comb}$ are found by maximizing CNR (left). Peak contrast values (right) are indicated at the respective optimal flip angles (40, 5, 15)°. PDSSFP achieves the highest peak contrast. (T1/T2=5)

Conclusion: We have developed a fast, 3D, motion-insensitive sequence for positive-contrast imaging that achieves robust water and fat suppression. The high peak contrast and background suppression of PDSSFP were demonstrated through simulation and phantom experiments. Further in vitro and in vivo experiments will be conducted to test the performance of PDSSFP for tracking SPIO-labeled cells.

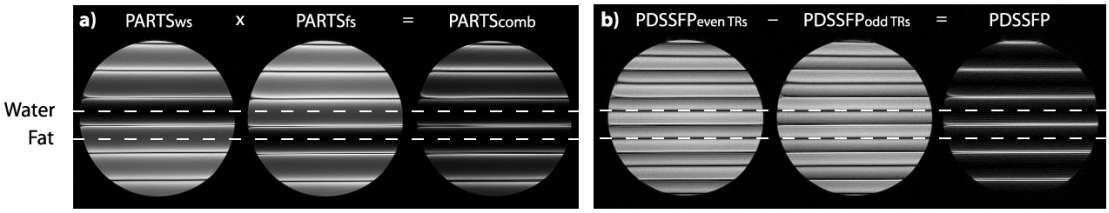

Figure 4. A ball phantom was scanned with a vertical field gradient. PARTS **(a)** nulls either water (left) or fat (center). The product image (right) nulls both resonances. PDSSFP **(b)** component images acquired in even (left) and odd (center) TRs are subtracted to yield the PDSSFP spectrum (right), which nulls water and fat resonances.

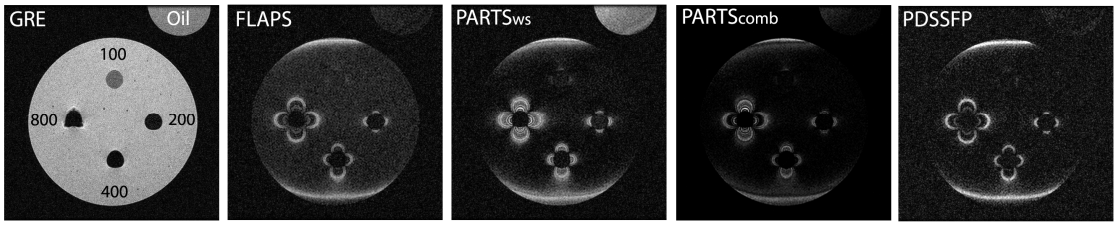

Figure 5. A gel phantom with 100, 200, 400, and 800 µg/mL concentrations of SPIO and an oil phantom were imaged with GRE, FLAPS, PARTS, and PDSSFP. PDSSFP generates large signal near SPIO regions and has better water and fat background suppression than FLAPS and $PARTS_{ws}$ (equal windowing: FLAPS, PARTS, PDSSFP).

References:
1. Dharmakumar R, *et al.* Phys Med Biol 51: 4201-4215, 2006.
2. Çukur T, *et al.* MRM 63: 427-437, 2010.
3. Overall W, *et al.* Proc. 16th ISMRM: 1445, 2008.
4. Patil S, *et al.* Eur Radiol, 2010.